

# Numerical study of the magnetorotational instability in weakly magnetised accretion disks

## Resolution dependence of the Shakura–Sunyaev $\alpha$

P. J. Käpylä and M. J. Korpi

Astronomy Division, Department of Physical Sciences, University of Oulu, PO BOX 3000, 90014 University of Oulu, Finland

Received ; accepted

**Abstract.** In this letter, we present numerical calculations made to investigate the possible resolution dependence of the Shakura & Sunyaev (1973) viscosity parameter  $\alpha$  from local magnetohydrodynamic simulations of the magnetorotational instability (MRI). We find that the values of  $\alpha$  do indeed depend significantly on the numerical resolution but also that when the highest resolutions attainable by the computational resources available are used, the growth of the  $\alpha$ -parameter seems to saturate. The values of  $\alpha$  are at most of the order of  $10^{-3}$ , which indicates that the sole presence of turbulence due to dynamo generated magnetic field in the disk is not enough to reproduce  $\alpha$ s of the order unity which could explain some observational results (e.g. Cannizzo 1993).

**Key words.** accretion disks – instabilities – magnetohydrodynamics

### 1. Introduction

The biggest problem in the theory of accretion disks has been the lack of knowledge of a widely applicable physical process which could reproduce the observed effective angular momentum transport. A decade ago, the magnetorotational instability was realised to have significance in the context of accretion disks (Balbus & Hawley 1991). The MRI was seen to excite and sustain turbulence giving rise to turbulent viscosity and outward angular momentum transport in local MHD calculations (e.g. Hawley et al. 1995, 1996; Brandenburg et al. 1995, 1996; Stone et al. 1996).

The efficiency of this process can be measured in terms of the Shakura & Sunyaev  $\alpha$ -parameter which parametrises the turbulent viscosity as  $\nu_t = \alpha c_s H$ , where  $c_s$  is the sound speed, and  $H$  the height of the disk. The above parametrisation was made assuming the motion of the gas to be subsonic and that the turbulent eddies are smaller than the disk height, resulting in  $\alpha$  as a dimensionless number whose values vary between zero and one. The interpretation of the lightcurves of some dwarf novae indicates that the value of  $\alpha$  should be of the order  $10^{-2}-1$  (e.g. Cannizzo 1993).

However, in the aforementioned numerical studies the values of  $\alpha$  have been at least an order of magnitude too low to account for the observational results. On the other hand, the numerical resolution was seen to affect the values of  $\alpha$  (e.g. Brandenburg et al. 1996; Miller & Stone 2000). Doubling the resolution increased the value of  $\alpha$  by a factor of  $\sim 1.5$  in these studies. This possible dependence has not been studied systematically yet, casting some doubt that high enough  $\alpha$ s can be obtained from local MRI calculations. Therefore, the purpose of this paper is to perform the previously missing survey on the resolution dependence of the  $\alpha$ -parameter.

### 2. The MHD model

The computational domain in our calculations is a rectangular box with dimensions  $L_i$ ,  $i = x, y, z$ , at a radius  $R_0$  from the centre of rotation. The distance to the centre of force is large in comparison to the box dimensions (i.e.  $R_0 \gg L_i$ ), under which assumption new locally cartesian coordinates can be taken into use and the equations of motion can be linearised (e.g. Spitzer & Schwarzschild 1953). This simplification is usually referred to as the shearing box approximation, in which we solve a set of non-ideal MHD-equations in cartesian coordinates (see Caunt & Korpi 2001).

We apply small molecular viscosities everywhere and additionally artificial shock- and hyperviscosities in order

---

Send offprint requests to: P. J. Käpylä  
e-mail: Petri.Kapyla@cc.oulu.fi

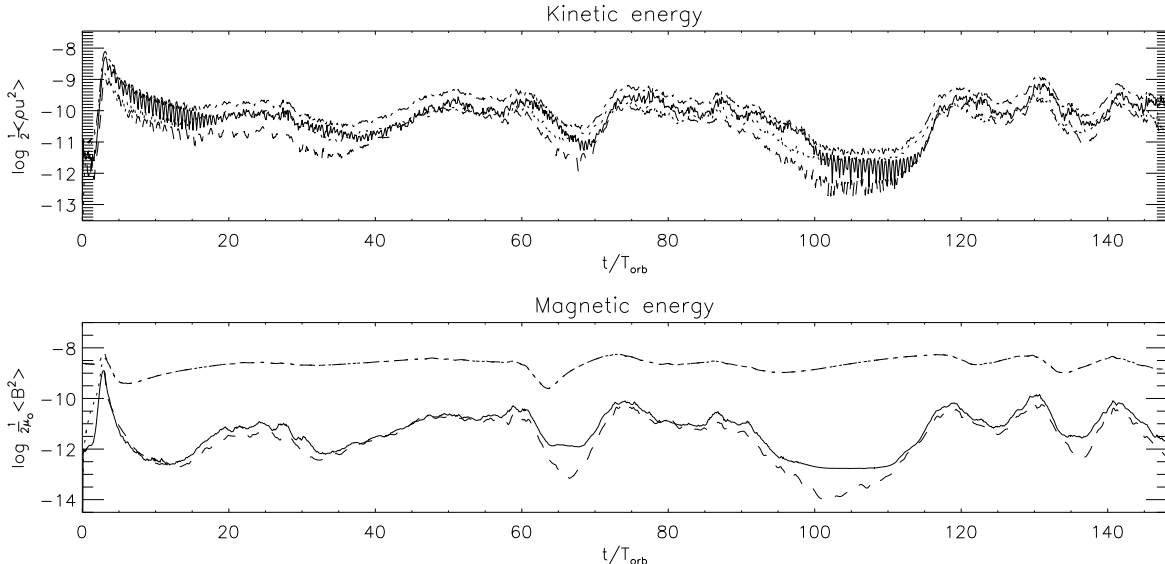


**Fig. 1.** Turbulent kinetic and magnetic energies from the run R1. The different components are denoted by solid (radial), dotted (azimuthal), and dashed (vertical) lines. The total energy is denoted by dash dotted line.

**Table 1.** The values of maximum and time averaged  $\alpha$ -parameters for the two sets of simulations. Time averages were taken up to  $13 T_{\text{orb}}$  (duration of the largest calculation), where  $T_{\text{orb}} = 2\pi/\Omega_0$  is the orbital period.

Run	Resolution	$\alpha_{\text{max}} [10^{-3}]$	$\langle \alpha \rangle_t [10^{-4}]$
T1	$15 \times 15 \times 31$	2	3
T2	$31 \times 31 \times 63$	13	10
T3	$47 \times 47 \times 95$	22	16
T4	$63 \times 63 \times 127$	23	32
T5	$95 \times 95 \times 191$	32	39
T6	$127 \times 127 \times 255$	28	41
R1	$31 \times 31 \times 63$	14	7
R2	$47 \times 47 \times 95$	16	18
R3	$63 \times 63 \times 127$	32	26

to resolve shocks and (unphysical) small scale oscillations, respectively. The artificial viscosities also serve the purpose of stabilising the numerics.

We adopt periodic boundary conditions in the radial and azimuthal directions, and closed insulating stress free boundaries in the vertical direction. The radial boundary takes into account the basic shear flow. Numerical implementation of the model described above is presented in the paper by Caunt & Korpi (2001).

### 3. Physical setup

We adopt the same dimensionless quantities as Brandenburg et al. (1995), i.e. length is measured in units of the initial density scale height  $[x] = H_0$ , time in units of  $[t] = (GM/H_0^3)^{-1/2}$ , and the density in units of  $[\rho] = \rho_0$ , the initial density at the midplane of the disk. The unit of magnetic field will then be  $[B] = [u](\mu_0 \rho_0)^{1/2}$ , where  $[u] = [x]/[t]$ . Dimensionless quantities are obtained by prescribing

$$H_0 = GM = \rho_0 = \mu_0 = 1. \quad (1)$$

Initially the disk is in hydrostatic equilibrium which yields a Gaussian density stratification

$$\ln \rho = \ln \rho_0 - \frac{z^2}{H_0^2}. \quad (2)$$

The initial magnetic field configuration is a sinusoidally distributed vertical field in the radial direction giving a zero net field. In terms of the vector potential this configuration can be represented as

$$\mathbf{A} = \frac{L_x}{2\pi} B_0 \cos\left(\frac{2\pi x}{L_x}\right) \hat{y}, \quad (3)$$

where  $B_0$  is calculated from the plasma beta,  $\beta = 2\mu_0 p/B_0^2$ , which has an initial value of 100 in the mid-plane of the disk. Random velocity perturbations of the order  $10^{-3} c_s$  were added in the velocity field to start up the instability.

### 4. Calculations

Two sets of calculations were made, differing in the box size. The numerical resolution was varied systematically, see Table 1 for complete details. In the R-set the used box size was the standard  $1 \times 2\pi \times 4$  in units of the initial density scale height  $H_0$ , as used by e.g. Hawley et al. (1995) and Brandenburg et al. (1995) to be able to compare the results with previous studies and thereby validate the code. In the T-set the smallest box size in which the MRI was still seen to be active and where the effects of the boundaries were not yet significant, namely  $1 \times 1 \times 2$ , was chosen in order to achieve the best possible spatial resolution. The lowest resolution runs were advanced up to  $\sim 150$  orbits, whereas the largest calculation could only be continued until 13 orbits in a reasonable amount of time. The duration of the largest calculation determined the length of the time average for the energies and the  $\alpha$ -parameter. In the calculations we systematically increase the resolution keeping the box size and other parameters fixed, and

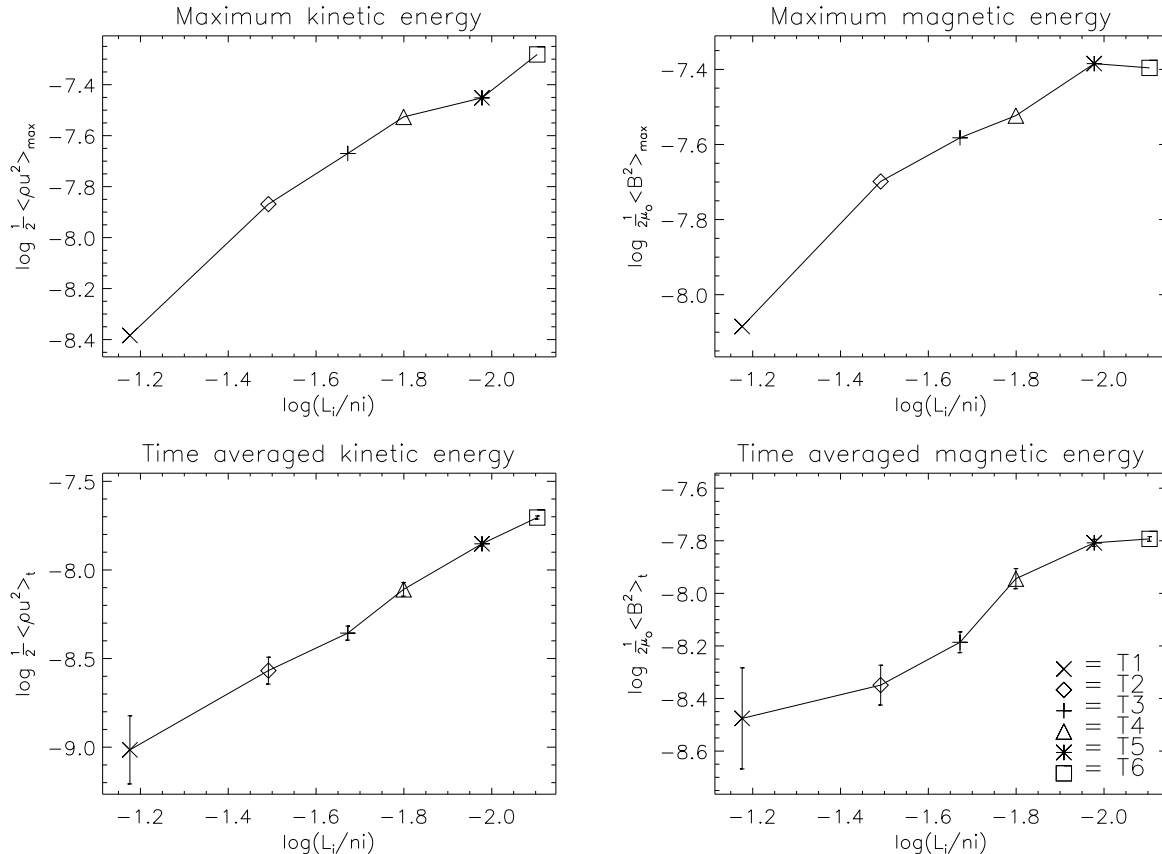


**Fig. 2.** Maximum and time averaged energies as a function of mesh size,  $\Delta_i = L_i/ni$ , where  $ni$  is the number of gridpoints and  $i = x, y$ , or  $z$ . The errorbars are given by a constant factor divided by the number of datapoints used in the calculation.

calculate the resulting Shakura–Sunyaev  $\alpha$ -parameter in the following two ways. Firstly, we calculate  $\alpha$  using the Maxwell and Reynolds stresses (see e.g. Brandenburg et al. 1995)

$$\alpha_{\text{stress}} = \frac{\langle \rho u_x u_y \rangle - \mu_0^{-1} \langle B_x B_y \rangle}{\frac{3}{2} \Omega_0 c_{s0} H_0 \langle \rho_0 \rangle}. \quad (4)$$

Secondly, we use the rate of dissipation

$$\alpha_{\text{diss}} = \frac{(\frac{d}{dt} \langle \rho e \rangle)_{\text{diss}}}{(\frac{3}{2} \Omega_0)^2 c_{s0} H_0 \langle \rho_0 \rangle}. \quad (5)$$

In Eqs. (4) and (5) the square brackets denote volume averages, and we use the initial values of density, sound speed and density scale height as the normalisation factor. As the values of  $\alpha$  from both methods coincide rather well, in the following we give only results from the first method. It is worth noting that the values of  $\alpha$  calculated in this way are smaller than the values of e.g. Hawley et al. (1995, 1996) by a factor of  $3/\sqrt{2}$  due to different normalisation factors.

## 5. Results

The overall behaviour of the system is clearly visible from Fig. 1 where we plot the kinetic and magnetic energies for the run R1. The behaviour of the energies in the higher

resolution simulations is very similar to the run R1, except that the energies are growing with resolution, see Fig. 2. After the initial exponential growth, the energies saturate into a self-sustained turbulent state. Although large fluctuations are seen, no persistent decay or growth is seen after about five orbits. The initially weak magnetic field is amplified considerably due to dynamo action which leads into a configuration where the field is strongly dominated by the azimuthal component, followed by significantly weaker radial and vertical components. The behaviour of the magnetic energy is very similar to the earlier studies (e.g. Brandenburg et al. 1995). The kinetic energy, however, is slightly dominated by the radial component in our simulations, whereas in some earlier works the azimuthal component has also dominated the kinetic energy. Even though the magnetic energy is at all times larger than the kinetic energy, the system is dominated by thermal energy which is usually of the order of  $\sim 100$  times larger than the magnetic energy. This causes the ratio of thermal to magnetic pressure to be such that the MRI is active at all times in the simulations.

Other characteristic numbers describing the system include the ratio of the Maxwell and Reynolds stresses, which are the main transport terms extracting energy from the Keplerian flow and transforming it into turbulent energy. In previous studies this ratio has been between 3 and 6. The value found in our simulations is close to 3,

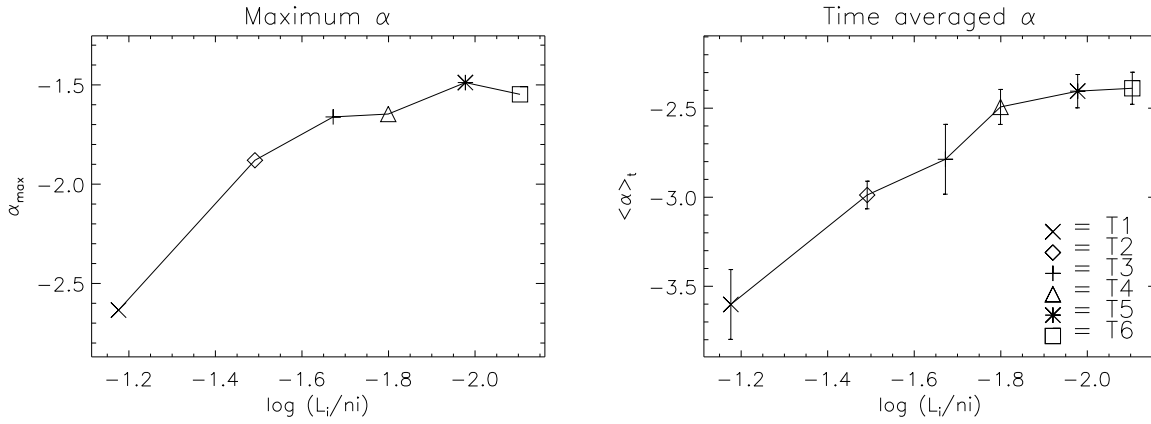


**Fig. 3.** Time averages of the  $\alpha$ -parameter as a function of mesh size,  $\Delta_i$ , where  $i = x, y$ , or  $z$ .

being in satisfactory agreement with the previous results. Although the results are not exactly identical to the earlier ones, the differences are not huge, and the basic characteristics can be well described by our model, indicating that it is valid.

The maximum and time averaged energies as functions of the mesh size,  $\Delta_i = L_i/ni$ , for the T-set are shown in Fig. 2. The maximum and time averaged kinetic energies both seem to continue almost linear growth beyond the resolutions investigated here, whereas the magnetic energies seem to saturate at the highest resolutions. A very similar trend was also found in the R-set (not shown), which indicates that the small box calculations are a valid tool in the study of resolution dependencies.

In Fig. 3 the maximum and time averaged  $\alpha$ -parameters as functions of mesh size are shown for the T-set of runs. The actual numerical values of  $\alpha$  are given in Table 1. As can be seen from this table for the R-set, doubling the resolution (from R1 to R3), the value of  $\alpha$  increases by a factor of  $\sim 3$ , which is even more dramatic than in previous studies (e.g. Brandenburg et al. 1996). In the T-set, the strong growth seen in the lowest resolutions seems to stop when resolution is increased further from the run T4. For the largest calculations,  $\alpha$  is almost constant. The largest values of time averaged  $\alpha$  we obtained were of the order of 0.004 which are roughly two orders of magnitude too low to account for the aforementioned observational results of dwarf novae.

## 6. Conclusions

In this letter, we have numerically investigated the resolution dependence of the Shakura & Sunyaev  $\alpha$ -parameter from a local MHD model of a weakly magnetised accretion disk where the MRI is acting. We find that the numerical resolution affects the energies and the values of  $\alpha$  significantly at lower resolutions. However, the strong growth of magnetic energy stops at the highest resolutions indicating that the Maxwell stress cannot extract more energy from the Keplerian shear flow when the resolution is increased which is also reflected in saturating trend seen in the values of  $\alpha$ . As the largest values of  $\alpha$  obtained in this study were only of the order  $10^{-3}$ , the obvious conclusion

is that it is not possible to obtain high enough  $\alpha$ s due to the MRI, at least not from local restricted models as the one studied here. There are, however, recent global studies of the MRI (e.g. Hawley 2001), which models exhibit large scale wave phenomena producing significantly higher values of  $\alpha$  (of the order  $\sim 0.1$ ).

Another hydromagnetic instability, namely the accretion ejection instability (AEI), investigated by Caunt & Tagger (2001) has recently been identified as a source of angular momentum transport, producing similar physical characteristics (spiral waves and comparable values of  $\alpha$ ) as the global MRI simulations, but which instability cannot operate without a fairly strong magnetic field. The AEI cannot generate this field by itself so it has to originate either from an external source or be generated by some intrinsic dynamo process, such as the one caused by the MRI. This suggests that the MRI is still a viable candidate to be responsible for the angular momentum transport (possibly indirectly via the AEI) in accretion disks and that it is the restricted geometry of the local models behind the too small values of  $\alpha$ .

*Acknowledgements.* The calculations were carried out using the supercomputers hosted by *CSC-Scientific Computing Ltd.*, Espoo, Finland. The authors wish to thank Prof. Axel Brandenburg for his valuable comments.

## References

- Balbus, S. A., & Hawley, J. F. 1991, *ApJ*, 376, 214
- Brandenburg, A., Nordlund, Å., Stein, R. F., & Torkelsson, U. 1995, *ApJ*, 446, 741
- Brandenburg, A., Nordlund, Å., Stein, R. F., & Torkelsson, U. 1996, *ApJ Lett.*, 458, L45
- Cannizzo, J. K. 1993, *ApJ*, 333, 227
- Caunt, S. E. & Korpi, M. J. 2001, *A&A*, 369, 706
- Caunt, S. E. & Tagger, M. 2001, *A&A*, 367, 1085
- Hawley, J. F., Gammie, C. F., & Balbus, S. A. 1995, *ApJ*, 440, 742
- Hawley, J. F., Gammie, C. F., & Balbus, S. A. 1995, *ApJ*, 464, 690
- Hawley, J. F. 2001, *ApJ*, 554, 534
- Miller, K. A. & Stone, J. M. 2000, *ApJ*, 534, 398
- Shakura, N. I., & Sunyaev, R. A. 1973, *A&A*, 24, 316
- Spitzer, L, jr, & Schwarzschild, M. 1953, *ApJ*, 118, 106

Stone, J. M., Hawley, J. F., Gammie, C. F., & Balbus, S. A.  
1996, ApJ, 463, 656